Water Research 206 (2021) 117756

Contents lists available at ScienceDirect

Water Research

journal homepage: www.elsevier.com/locate/watres

Quantification of DOM effects on tetracyclines transport during struvite recovery from swine wastewater

Xuewei Huang [a,b], Zhi-Long Ye [a,*], Jiasheng Cai [a], Lifeng Lin [a]

[a] Key Laboratory of Urban Pollutant Conversion, Institute of Urban Environment, Chinese Academy of Sciences, No. 1799 Jimei Road, Xiamen, Fujian 361021, China
[b] University of Chinese Academy of Sciences, Beijing 100049, China

ARTICLE INFO

Keywords:
Phosphorus recovery
Antibiotics
Dissolved organic matters
Quantification
Struvite

ABSTRACT

Struvite ($MgNH_4PO_4{\cdot}6H_2O$) recovered from livestock wastewater may impose a pharmacological threat to the environment, due to the extensive existence of antibiotics in the wastewater. In this study, tetracyclines (TCs) were selected as the typical antibiotics, and the individual processes of dissolved organic matters (DOM) evolution and their effects on TCs migration in struvite recovery from swine wastewater were discriminated and quantified. Results revealed that TCs transport was contributed by the adsorption of pure struvite crystals, struvite adsorbing DOM-TCs complex and DOM aggregation, which occupied 2.29–6.53%, 23.53–34.66%, and 59.09–74.19% of the total TCs migration amounts, respectively. A tangential flow filtration system was employed to divide DOM into five fractional parts on the basis of molecular weight cut-offs. Experimental results indicated that under alkaline conditions of struvite crystallization, DOMs with larger molecular weights, hydrolyzed to DOMs with smaller molecular weights, which consequently promoted TCs re-distribution in DOMs from higher molecular weights to those with lower molecular weights. Furthermore, a distribution model was developed to characterize TCs transport in struvite recovery by describing TCs distribution among various phases, including struvite adsorption, DOM-TCs complexing, DOM aggregation, and free state in the solution, respectively. These outcomes provided new understanding on DOM evolution and effects on antibiotics transport in phosphate recovery from wastewater.

1. Introduction

Rapid urban expansion and economic development contributed to the prosperity of the pig industry. According to the China Statistical Yearbook 2020, there has been more than 544 million pigs produced annually in China (NBSPRC, 2020). Consequently, the enormous risk to the environment caused by a large amount of phosphorus and ammonium discharged from swine wastewater has attracted widespread attention (Vanotti et al., 2017). From another aspect, swine wastewater enriched nitrogen and phosphorus are suitable for struvite ($MgNH_4PO_4{\cdot}6H_2O$) recovery (Li et al., 2021a; Muhmood et al., 2021). As a superior slow-release fertilizer, struvite can be used directly on agricultural planting (Lu et al., 2021).

Presently, intensive pig farming widely uses veterinary antibiotics to promote animal growth and prevent animal diseases (Cheng et al., 2020; Zhang et al., 2018). According to the literature, the worldwide use of veterinary antibiotics will increase by 67% between 2010 and 2030, and among them tetracyclines (TCs) are one type of the leading veterinary antibiotics (Cheng et al., 2020; Van et al., 2020). These antibiotics are hardly absorbed by animal guts, and are discharged into the feces and urine (Wang et al., 2019). Consequently, the persistent exposure of antibiotics in the environment leads to the spread of antibiotic resistance in the environmental media, which poses health risks to the human body and the ecological environment (Xu et al., 2021). It should be noted from our previous studies that the application of struvite fertilizer recovered from swine wastewater increased the diversity and abundance of antibiotic resistance genes in the soil, and thereby promoting the spread of antibiotic resistance in the food chain and threatening human health (Cai et al., 2020; Chen et al., 2017a).

According to our previous works, struvite crystallization in synthetic wastewater would trigger TCs transport from the liquid to the final solids, and the maximum adsorption capacities of TCs were ranging from 1494.7g to 2160.0 μg/kg (Ye et al., 2017). As to real swine wastewater, it contains a significant amount of dissolved organic matters (DOM), such as humic acid, fulvic acid, and proteins (Zhou et al., 2019; Zeng et al., 2017). These organic components have various function groups,

* Corresponding author.
E-mail address: zlye@iue.ac.cn (Z.-L. Ye).

https://doi.org/10.1016/j.watres.2021.117756
Received 20 July 2021; Received in revised form 28 September 2021; Accepted 8 October 2021
Available online 14 October 2021

including acidic moieties, polysaccharides, fatty acids, and long aliphatic side chains, which have the capability of determining the migration behavior of TCs (Li et al., 2021b; Safiur Rahman et al., 2013; Wang et al., 2020). We did find that the presence of DOM can promote the transfer of TCs from the aqueous phase to struvite solid, and the DOM with higher molecular weight (HMW) plays an important role due to its higher aromaticity and more functional groups (Lou et al., 2018; Ye et al., 2020). In addition, since struvite crystallization was carried out under alkaline conditions, HMW DOM were hydrolyzed into ones with low molecular weights (LMW) (Xu et al., 2018; Ye et al., 2020). This phenomenon might result in the redistribution of TCs among various DOM components. Besides, struvite precipitation would also trigger DOM evolution with DOM adsorption by struvite crystals and DOM aggregation, and consequently resulted with more TCs migrating from the aqueous phase to the recovered struvite products (Ye et al., 2020). However, few studies have been devoted to quantifying the specific effects of DOM evolution on TCs transport. This is very important since phosphorus recovery has been widely applied in wastewater treatment at full scales. The outcomes of this study can provide the quantitative information of antibiotic transport in phosphorus recovery, which will undoubtedly be helpful to develop the methods of antibiotic control in phosphorus recovery from wastewater.

In the present study, the sub-processes of DOM evolution in struvite crystallization, including hydrolysis, adsorption, and aggregation, were clarified and quantified, and their contributions to TCs transport were determined. A tangential flow filtration system was employed to fractionate DOM into several individual parts based on the molecular weight cut-off, and their interactions with TCs before and after hydrolysis under alkaline conditions were evaluated. A series of subsequent experiments were conducted to determine the TCs transport driven by struvite adsorption, DOM hydrolysis, DOM aggregation, and DOM complexing with TCs, respectively. And a distribution model between struvite, DOM and TCs in the process of struvite crystallization were also discussed.

2. Materials and methods

2.1. Chemicals and standards

Three individual TCs standards, including tetracycline (TC), doxycycline (DXC), and oxytetracycline (OTC) were obtained from the Alladin Ltd. USA. The properties of these tetracylines were listed in Table S1. Tetracycline-D6 (80% purity) was purchased from Toronto Research Chemicals Inc (North York, Canada), used as an internal standard. OasisHLB cartridges (size of 200 mg, 6 mL) which were used for sample pretreatment, were bought from Waters (Milford, USA).

Raw swine wastewater was obtained from the digested effluent of a treatment process in an intensive pig farming plant, located in Zhangzhou City, China. Centrifugation at 7500 rpm for 15 min was firstly conducted to remove suspended organics (Ben et al., 2013). After the centrifugation, the parameters of the wastewater were analyzed, as displayed in Table S2. As to TCs, their concentrations respectively were (μg/L): OTC 15.33±2.46, TC 17.16±2.13, DXC 14.23±0.99.

Other chemicals used for struvite crystallization, including $(NH_3)_2HPO_4$, $MgCl_2{\cdot}6H_2O$ and NaOH, were all chemical pure and supplied by Xi Long Co. (China). Ultrapure water was generated by a Milli-Q water purification system (18.2 ΩM·cm) from Millipore (Boston, USA).

2.2. DOM fractionation

As described in the literature (Zhao et al., 2021), DOM with different molecular weights might display different effects on the environmental behavior of antibiotics. Therefore, a tangential flow filtration (TFF) system (PALL Minimate, Pall Life Sciences Co., USA), described in our previous study was adopted to fractionate DOM into several fractional DOMs (FDOM) with four different molecular weight cut-offs (Fig. S1), i.e. 100 kDa–0.45 μm (FDOM1), 30–100 kDa (FDOM2), 5–30 kDa (FDOM3), 1–5 kDa (FDOM4) and < 1 kDa (FDOM5), respectively (Lou et al., 2018). After every fractionation sub-process, the DOM recovery (as%DOC) was calculated by measuring the quantity of dissolved organic carbon in the retentate and filtrate before and after each fractionation filtration (Kitis et al., 2001; Moody, 2020). During the fractionation process, the DOM recovery values ranged from 82.37% to 101.07%.

2.3. Experimental design and setup

In order to quantify the effects of DOM evolution on TCs transport during struvite recovery from wastewater, blank control test and a series of subsequent experiments were conducted, respectively.

2.3.1. Changes of TCs and DOM in struvite precipitation

Blank control experiment was carried out to figure out the overall changes of TCs and DOM during struvite recovery from real wastewater. To amplify the effects of TCs migration, a certain amount of TCs were dosed into the liquid to increase the initial TCs concentrations to 81.49–158 μg/L. Then the wastewater was subjected to struvite precipitation, where pH was kept at 9.0 and Mg:P molar ratio was set at 1.2:1, respectively. After 60 min agitation, the mixture was settled down for 60 min. The solid precipitates were collected for further analyses, and DOM variation in the aqueous phase and TCs contents in the solids were measured.

2.3.2. Effects of DOM evolution on TCs transport

With regard to DOM evolution during struvite crystallization, it possessed several sub-processes, including hydrolysis under alkaline conditions, adsorption by struvite crystals and aggregation, respectively. In order to screen out the specific functions of DOM evolution on TCs transport, a series experiments were designed to separate each step of DOM evolution. Before the experiments, the wastewater was firstly diluted 5 times so as to reduce phosphate concentrations and prevent the disturbance of struvite precipitation.

(1) DOM hydrolysis and TCs re-distributions under alkaline conditions

For struvite recovery, pH value should be kept at 9.0–10.5, which would induce DOM hydrolysis (Ye et al., 2017). In this study, DOM hydrolysis and its influence on TCs distribution were examined by setting a comparison between initial wastewater and the one with pH adjusting to 9.0. After 60 min agitation, water samples were withdrawn for DOM fractionation and parameter analyses, including TOC, fluorescence and ultraviolet-visible spectra, antibiotics. A TFF system was also applied to investigate the variation of TCs concentration among various FDOMs before and after hydrolysis.

(2) DOM-TCs adsorption onto struvite crystals

After hydrolysis, as described in the above section, the wastewater was subjected to struvite crystals adsorption, which focused on the aqueous TCs deficit contributing by DOM-TCs complexation. In this section, a series of synthetic wastewater containing certain amounts of TCs was firstly prepared, with their concentrations referencing to those in the real wastewater. Struvite crystals were sufficiently produced by using deionized water and separated by centrifugation, and then divided equally into two groups. Each group consisted of different struvite concentrations, i.e. 3, 6, 9, 12, 15 mmol/L, respectively. For the first group, struvite crystals were dosed into the real wastewater for DOM-TCs adsorption, while the other group struvite particles were added in synthetic wastewater containing certain TCs amounts for comparison. All the vessels were shaken for 60 min following 120 min settling down, and the solids were collected by centrifugation. The supernatants were collected for the further subsequent processes, which would focus on the

effects of DOM aggregation on TCs migration.

(3) Effects of DOM aggregation on TCs transport

In this section, calculated amounts of TCs were dosed into the supernatant so as to keep the initial TCs concentrations similar to those before DOM-TCs adsorption. This was necessary since it could respectively quantify the contribution of DOM aggregation on TCs transport in struvite crystallization. After that, desired amounts of PO_4^{3-} (to reach 100 mg/L) were added into the liquid and Mg:P molar ratio was set at 1.2:1 to perform struvite precipitation. The recovered solids and liquid samples were withdrawn for further analyses.

2.4. Analytical methods

2.4.1. Regular methods

Regular parameters of the wastewater, including ammonium (NH_4^+-N), total nitrogen, phosphate (PO_4^{3-}-P) and total phosphorus were assayed by the standard methods (APHA). DOC was measured by using a TOC analyzer (TOC-Vcph, Shimadzu, Japan). Mg^{2+} and Ca^{2+}were conducted by the inductively coupled plasma optical emission spectroscopy (Optima 7000DV, PerkinElmer, USA). Anionic ions, including sulfate and nitrate, were measured by using chromatograph (Aquion ICS, Thermo Fisher, USA).

2.4.2. Tetracyclines assay

The determination of TCs was conducted by using the chromatography/tandem mass spectrometry (ABI3200 QTRAP, USA) combining with Phenomennex Kinetex Symmetry C18 column (2.1 mm × 50 mm) for identification and quantitation of TCs. The mass spectrometry system was installed with electrospray ionization (ESI) source and was operated with desolation temperature at 300 °C and capillary voltage 5.5 KV.

Before TCs determination, solid samples were firstly mixed with 10 mL 10% (v/v) HCl and sonicated for 20 min to dissolve struvite crystals. After that, for both solid and liquid samples were diluted to approximately 200 mL with phosphate buffered saline, and acidified to pH 2.8–3.2 by adding 10% (v/v) HCl. Oasis HLB cartridge (200 mg/6 mL, Waters, Milliford, USA) was then used to extract TCs from the samples, where the extraction processes have been described in our previous works (Ye et al., 2017; Huang et al., 2013). Subsequently, the Oasis HLB cartridges were rinsed with by certain amounts of acetone, methanol and Milli-Q water. The eluate was dried under a nitrogen stream at 35 °C. 20% (v/v) methanol was used to bring the final purified extract volume up to 1 mL. After 2 min of Vortex oscillation, the final extract was filtered through a 0.22 μm membrane and stored at −20 °C for further analysis.

Recovery rate, detection limits and the quantification for the instrument were determined by using calibration curves, which has been reported in our previous works (Ye et al., 2017). The recovery rates detected in the present study were displayed in Table S3.

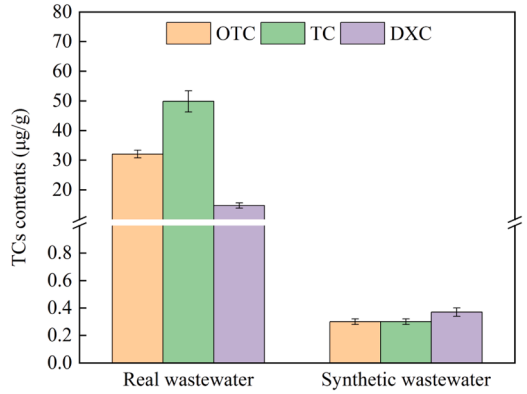

Fig. 1. TCs contents in struvite solids recovered from real wastewater and synthetic wastewater.

2.4.3. Spectrum analyses

Three-dimensional excitation (Ex) and emission (Em) matrix fluorescence (3DEEM) spectroscopy, which was applied to investigate the difference of DOM before and after struvite reaction, was detected by using a fluorescence spectrofluorometer (F-4600, Hitachi Co., Japan) equipped with a 150 W Xenon arc lamp as the light source. 3DEEM analysis scan rate was controlled at 1200 nm/min, with sampling interval at 5 nm on both Ex and Em. In addition Ex and Em slit bandwidths were set at 5 nm, and the scanning field was set at from 200 to 550 nm on excitation and emission spectra. Fluorescence regional integration (FRI) of the 3DEEM was further adopted to evaluate the variation of DOM components in the processes (Chen and Yu, 2020). Generally, 3DEEM was defined into five excitation-emission regions, depending on the fluorescence of model compounds (Table S4). In order to remove the background and Raman scatter, Fluorescence of Milli-Q water was subtracted from samples spectra(Chen et al., 2017c). The collected data were addressed by Origin 2021 (Origin Lab Inc., USA)

A spectrophotometer (DR5000, Hach, USA) was adopted to measure the UV–Vis absorbance between 200 and 400 nm. $SUVA_{254}$, as a parameter of representing the relative contents of aromatic structures in DOM, was described by the following equation:

$$SUVA_{254} = \frac{UV_{254}}{DOC} \times 100$$

Herein, UV_{254} (cm^{-1}) is absorbance at λ=254 nm, and DOC (mg/L) is dissolved organic carbon.

2.5. Distribution coefficient

It should be pointed out that during struvite precipitation TCs were distributed among four phases, including molecules sorbed to struvite crystals (K_{MAP}), molecules complexing with DOM (DOMs-TCs, K_{DOMs}), adsorbed onto struvite crystals, molecules complexing with DOM aggregated (DOMa-TCs, K_{DOMs}) and molecules freely dissolved in the solution. Therefore, the effects of DOM on TCs transport could be understood by examining TCs examining mass distribution among these phases, which could provide useful information for understanding TCs migration during phosphate recovery from wastewater. The following equations were used to determine TCs distribution coefficients, which were derived based on mass balance.

$$f_1 = \frac{K_{MAP}C_{MAP}}{K_{MAP}C_{MAP} + K_{DOMs}C_{DOMs} + K_{DOMa}C_{DOMa} + 1}$$

$$f_2 = \frac{K_{DOMs}C_{DOMs}}{K_{MAP}C_{MAP} + K_{DOMs}C_{DOMs} + K_{DOMa}C_{DOMa} + 1}$$

$$f_3 = \frac{K_{DOMa}C_{DOMa}}{K_{MAP}C_{MAP} + K_{DOMs}C_{DOMs} + K_{DOMa}C_{DOMa} + 1}$$

$$f_4 = \frac{1}{K_{MAP}C_{MAP} + K_{DOMs}C_{DOMs} + K_{DOMa}C_{DOMa} + 1}$$

$$K_{MAP}\ (L/kg) = \frac{\text{Struvite crystal TCs adsorption quantity (mg/kg)}}{\text{Struvite crystal amounts (mg/L)}}$$

$$K_{DOMs}\ (L/kg) = \frac{\text{DOMs} - \text{TCs adsorption quantity (mg/kg)}}{\text{DOMs adsorption quantity (mg/L)}}$$

$$K_{DOMa}\ (L/kg) = \frac{\text{Aggregation DOMa} - \text{TCs adsorption quantity (mg/kg)}}{\text{DOMa adsorption quantity (mg/L)}}$$

where f_1, f_2, f_3 and f_4 were coefficients of TCs distributing among struvite crystals, complexation with DOM adsorbed onto struvite crystals,

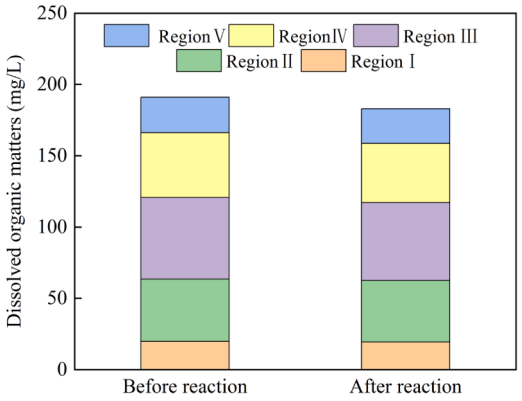

Fig. 2. Variation of different DOM components in swine wastewater before and after struvite precipitation. Region I, aromatic protein I; Region II, aromatic protein II; Region III, fulvic acid-like; Region IV, soluble microbial by-product-like; Region V, humic acid-like.

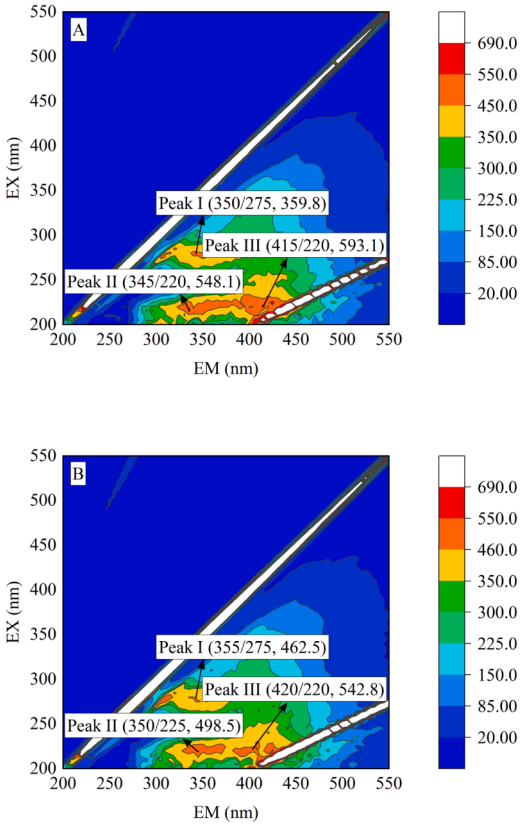

Fig. 3. Fluorescence spectra of DOM in swine wastewater before (A) and after (B) struvite reaction.

complexation with DOM aggregated and free molecule in the solution, respectively. K_{MAP}, K_{DOMs}, and K_{DOMa} were represented the respectively binding constants of TCs with struvite crystals, DOMs adsorption onto struvite crystals, and DOMa aggregation. C_{MAP}, C_{DOMs}, and C_{DOMa} was struvite crystal amounts, DOMs adsorption quantity and DOMa aggregation quantity.

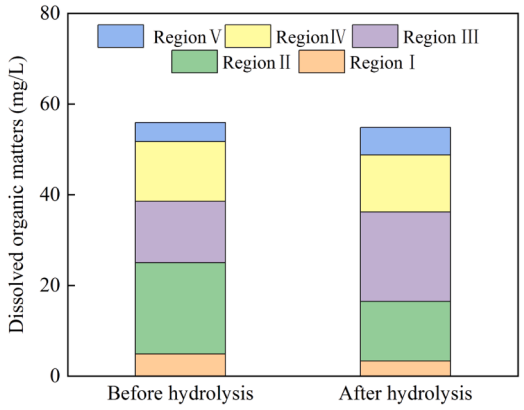

Fig. 4. FRI distribution of different DOM components in swine wastewater before and after hydrolysis under alkaline conditions. Region I, aromatic protein I; Region II, aromatic protein II; Region III, fulvic acid-like; Region IV, soluble microbial by-product-like; Region V, humic acid-like.

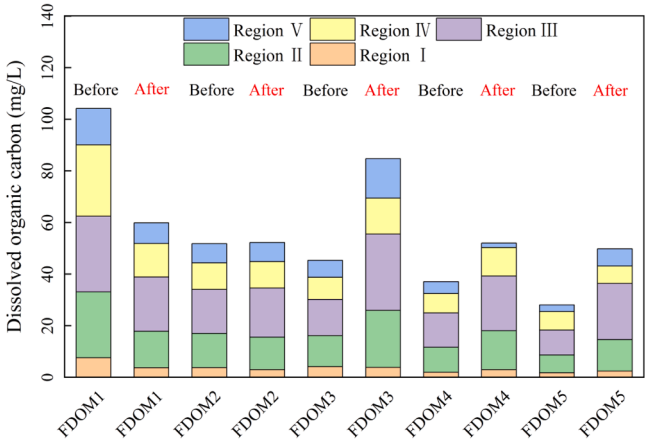

Fig. 5. FRI distribution of different DOM components in FDOMs of swine wastewater before and after hydrolysis under alkaline conditions. Region I, aromatic protein I; Region II, aromatic protein II; Region III, fulvic acid-like; Region IV, soluble microbial by-product-like; Region V, humic acid-like.

3. Result and discussion

3.1. Changes of TCs and DOM components in the process of struvite precipitation

As displayed in Fig. 1, TCs contents in the solids recovered from real wastewater (14.67–47.86 μg/g) were obviously higher than those recovered from synthetic wastewater (0.26–0.37 μg/g). To investigate the discrepancies of DOM components in struvite recovery process, the method of fluorescence regional integration (FRI) was employed. As shown in Fig. 2, the loss of DOC was about 4.60% of the total DOC in the liquid. In addition, Fig. 3 demonstrated the discrepancies of DOM fluorescence spectra before and after struvite crystallization, and shifts of different peak locations and intensity changes were observed. Peak intensity of Peak I was increased, while those of Peak II & III were decreased. These phenomena implied that DOM evolution could highly improve the migration of TCs from liquid phase to solid phase, as described in our previous works (Lou et al., 2018). This study focused on quantifying the functions of DOM evolution on TCs transport in struvite recovery.

Table 1
The changes of $SUVA_{254}$ before and after hydrolysis under alkaline conditions.

Term	$SUVA_{254}$ (L/(mg•m)) Before	After
FDOM1	1.31 ± 0.08	0.38 ± 0.02
FDOM2	1.34 ± 0.05	0.33 ± 0.02
FDOM3	1.05 ± 0.08	1.08 ± 0.04
FDOM4	1.04 ± 0.03	0.48 ± 0.05
FDOM5	0.88 ± 0.03	0.04 ± 0.00

3.2. Screening out the functions of DOM evolution on TCs transport

3.2.1. DOM hydrolysis and TCs re-distributions under alkaline conditions

According to literature, alkaline conditions can lead to obvious hydrolysis of DOM by ionizing the function group, such as carboxylic and phenolic acid groups, and dispersing the molecules due to electrostatic repulsion (Ma et al., 2019; Liu et al., 2020). In the present study, the changes of DOM components under alkaline conditions were assayed by 3DEEM. The results indicated that the concentrations of aromatic protein I and aromatic protein II decreased while the levels of fulvic acid-like and humic acid-like materials increased (Fig. 4). In addition, the discrepancies of fluorescence spectra, as displayed in Figs. S2 and S3, also supported DOM hydrolysis under alkaline conditions, where changes of peak shifts and intensity were detected.

In order to investigate the alternation of TCs distribution among various DOM components, a TFF system based on molecular cut-off was applied to fractionate DOM before and after hydrolysis into five fractional DOMs (FDOMs) of different Molecular weights. Fig. 5 demonstrated the variation of FDOMs under alkaline conditions. Except for FDOM1 reduction, the concentrations of FDOM3, FDOM4, FDOM5 increased 13%, 21% and 50% after hydrolysis, respectively. These suggested that FDOMs with lower molecular weights (LMW) were

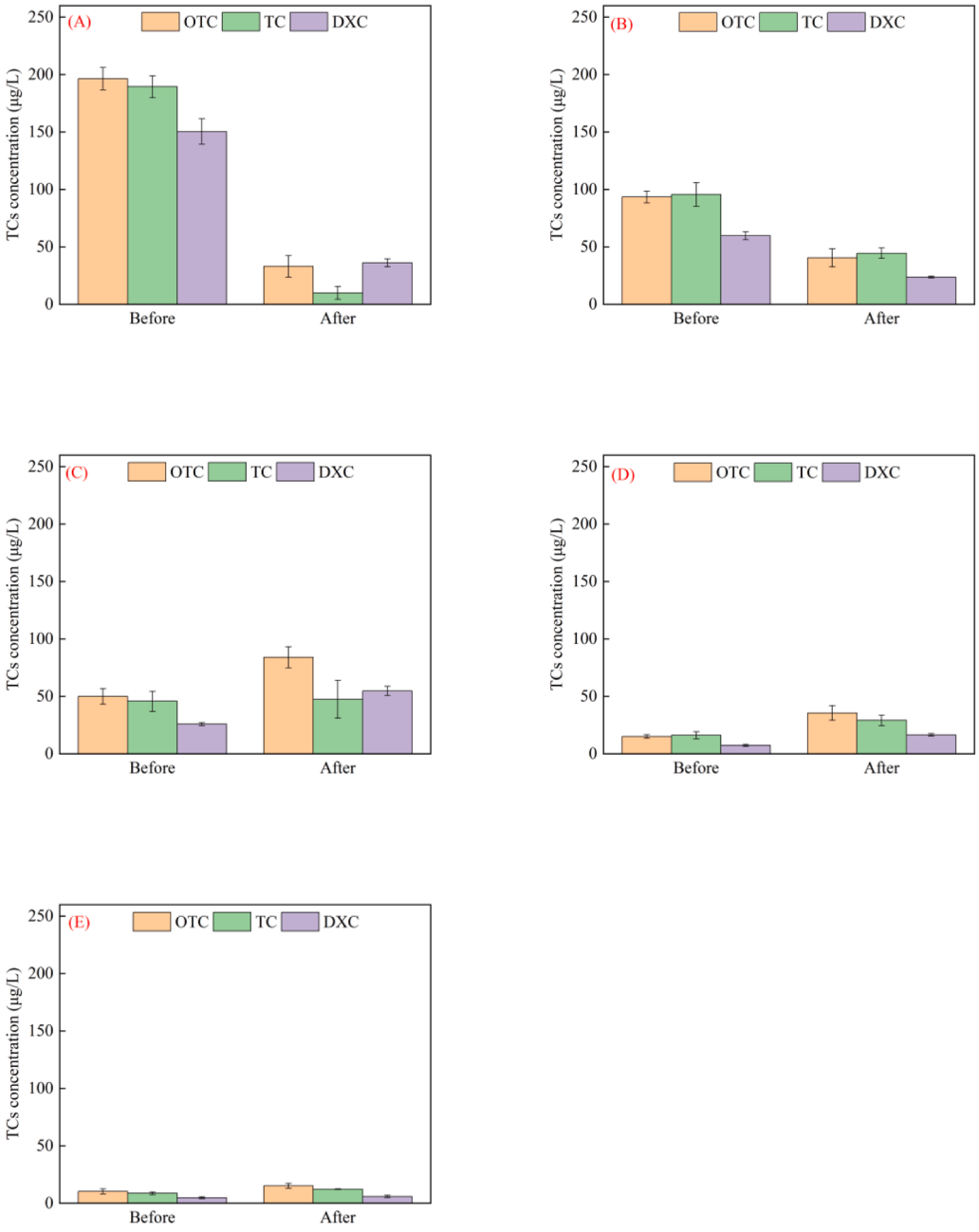

Fig. 6. The changes of TCs contents in FDOM1 (A), FDOM2 (B), FDOM3 (C), FDOM4 (D) and FDOM5 (E), before and after hydrolysis under alkaline conditions.

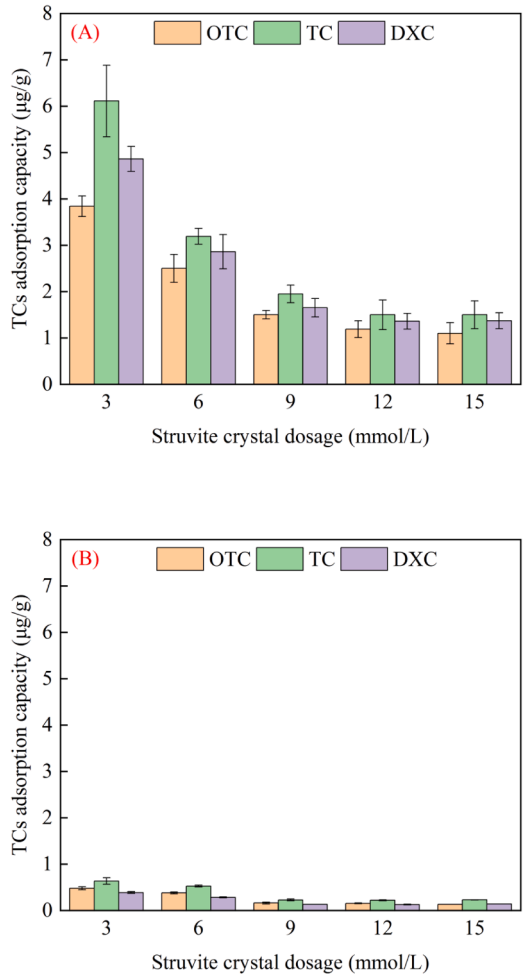

Fig. 7. TCs contents in the solid after adsorption by struvite crystals from real wastewater (A) and synthetic wastewater (B).

compensated by the hydrolysis of FDOMs with larger molecular weights. The $SUVA_{254}$ values of various FDOMs were calculated, which represented the relative contents of aromatic structures in DOM and could be used to evaluate the chelation is a parameter, which represented the relative contents of aromatic structures in DOM and could be used to evaluate the chelation potential with TCs. As summarized in Table 1, $SUVA_{254}$ values of FDOM1, FDOM2, FDOM4, FDOM5 were found to be significantly decreased, which indicated that the amounts of unsaturated carbon bonds and aromaticity was reduced after hydrolysis (Yuan et al., 2020).

Fig. 6 illustrated the variation of TCs distribution among various FDOMs during hydrolysis. It has been reported that FDOMs with higher molecular weights (HMW) had higher aromaticity with more acidic groups, fatty acids, long aliphatic side chains and polysaccharides, and could chelate with TCs more easily (Ma et al., 2013). This was also confirmed in the present study where TCs displayed stronger chelation capacities with HMW FDOMs before hydrolysis (Fig. 6). The sequence of chelating capacities of individual FDOMs with TCs was FDOM1 > FDOM2 > FDOM3 > FDOM4 > FDOM5, which largely matched with the sequence of $SUVA_{254}$ values (Table 1).

It was observed that after hydrolysis the concentrations of TCs chelating with FDOM1 and FDOM2 significantly decreased, while the amounts of TCs complexing with FDOM3, FDOM4 and FDOM5 increased 1.73–33.94 μg/L, 9.18–20.48 μg/L, 1.00–4.88 μg/L (Fig. 6), respectively. These results demonstrated that under the alkaline conditions of struvite precipitation, DOM hydrolysis promoted TCs redistributing from HMW FDOMs to LMW FDOMs. Further examination

Table 2
Regression analyses on TCs and DOC adsorbing by struvite crystals.

TCs	Regression equation	R^2
OTC	$y = 0.220x + 0.861$*	0.970
TC	$y = 0.214x + 1.393$	0.749
DXC	$y = 0.336x + 0.766$	0.815

* y, TCs adsorption by struvite crystals (μg/g); x, DOC adsorption by struvite crystals (mg/g).

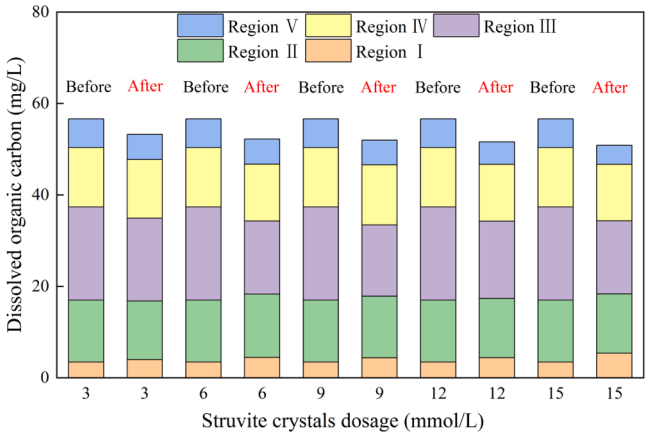

Fig. 8. FRI distribution of different DOM components in swine wastewater before and after DOM adsorption by struvite crystals. Region I, aromatic protein I; Region II, aromatic protein II; Region III, fulvic acid-like; Region IV, soluble microbial by-product-like; Region V, humic acid-like.

on the components of individual FDOM was conducted (Fig. 5), and results displayed that the concentrations of aromatic proteins I and II, fulvic acid-like materials in LMW FDOMs were raised, coupling with TCs increase in relevant smaller FDOMs. Previous research has revealed that higher pH would not only be in favor of HMW FDOMs to LMW FDOMs, while was effective at releasing protein-like, polysaccharide-like and fulvic acid-like materials from HMW FDOMs to LMW FDOMs (Chen et al., 2017b; Li et al., 2016), also as displayed in Fig. 5. Under such circumstances, the tricarbonyl group and phenolic diketone moiety of TCs were neutral or negative, and the dimethylamino group demonstrated a localized positive charge (Ding et al., 2013; Ye et al., 2017). Consequently, TCs were prone to chelate with protein-like, polysaccharide-like and fulvic acid-like materials (Fig. 5), since they had higher affinity capabilities with these DOM components (Bai et al., 2017). Therefore, the augment of TCs distribution in FDOM3, FDOM4 and FDOM5 was observed as shown in Fig. 6.

3.2.2. *DOM-TCs adsorption by struvite crystals*

The capacities of struvite crystals adsorbing TCs under synthetic and real wastewater were compared. As shown in Fig. 7. TCs levels in the struvite solids obtained from real wastewater were dramatically higher than those from synthetic wastewater. The results indicated that DOM-TCs complex could promote the adsorption of TCs onto struvite crystals due to the co-adsorption (Guillossou et al., 2020). Besides, in case the dosage of struvite crystals increased, the TCs adsorption capacities were declined since struvite crystals could provide more functional sites for TCs and DOM sorption (Wang et al., 2020). It should be pointed that TCs adsorbed by pure struvite in synthetic wastewater occupied 8.87–20.40% of the total TCs adsorption amount in real wastewater. Further investigation was conducted on evaluating the relation between TCs and DOM simultaneously adsorbing onto struvite crystals. As illustrated in Table 2, a linear relationship was detected with the R^2 values ranging from 0.749 to 0.970. Similar results of TCs levels coupling with the enhancement of TOC contents in the struvite products

Table 3
TCs residue detected in the struvite products contributed by DOM aggregation. Initial water of sample 1–5 was the supernatants obtained in Section 3.2.2 by adsorption of 3, 6, 9, 12, and 15 mmol/L struvite crystals, respectively.

TCs	OTC (μg/g)	CTC (μg/g)	DXC (μg/g)
Sample 1	10.13±0.38	10.09±0.62	11.67±0.42
Sample 2	10.55±1.12	9.2±0.54	11.49±0.53
Sample 3	11.91±0.49	10.11±0.65	10.79±1.46
Sample 4	10.92±0.77	10.03±0.59	10.03±0.38
Sample 5	11.63±0.82	10.15±0.29	11.29±0.38

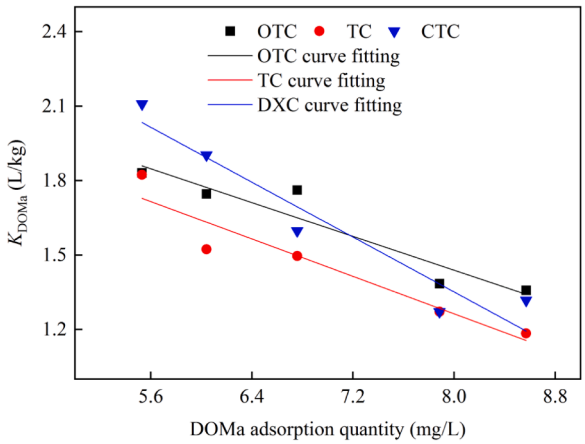

Fig. 9. Relationship between Aggregation K_{DOMa} and DOMa adsorption quantity.

were reported by previous research (Lou et al., 2018; Ye et al., 2018).

The fluorescence regional integration (FRI) method was employed to evaluate the variation of various FDOM components before and after struvite adsorption. It was obvious that the dosage of struvite crystals resulted in the loss of aqueous DOC (Fig. 8). With regard to specific FDOM components, the reduction of aromatic protein II (Region I), fulvic acid-like (Region III) and humic acid -like (Region V) materials in the liquid were observed after struvite adsorption.

3.2.3. *Effects of DOM aggregation on TCs transport*

According to previous studies, struvite crystallization could ignite DOM aggregation and therefore trigger TCs migration (Ye et al., 2020). To clarify the functions of DOM aggregation on TCs transport, the supernatants obtained in Section 3.2.2 were directly subjected to struvite crystallization. Desired amount of TCs and phosphate were added into the liquid to keep initial TCs and phosphate concentrations, respectively at the same levels. In this section, the functions of DOM hydrolysis and adsorption on TCs migration should not be in consideration, since the supernatants have undergone two stages (Sections 3.2.1 and 3.2.2), i.e. DOM hydrolysis (TCs re-distribution) and struvite crystals sorbing DOM (DOM-TCs adsorbing by struvite crystals), respectively.

The amounts of TCs residues in the recovered solids ascribed to DOM aggregation (Table 3) were measured, which displayed 3.27–6.10 times higher than those contributed by struvite adsorbing DOM-TCs (Fig. 7). As described by literature, significant changes of ion strength or salinity could trigger DOM aggregation (Baalousha et al., 2006), which therefore could enhance the complex interactions of DOM with organic contaminates due to the increase of zeta potential and the formation of both hydrophobic and hydrophilic domains (Gu et al., 2007; Pan et al., 2008).

According to our previous research, struvite precipitation would promote the compression on the electrical layer of DOM molecules, and the precipitated DOM fractions exhibited direct effects on TCs residue in the recovered products (Lou et al., 2018). In this section, a decrement of aqueous TOC from 53.24 to 50.84 mg/L was detected among the

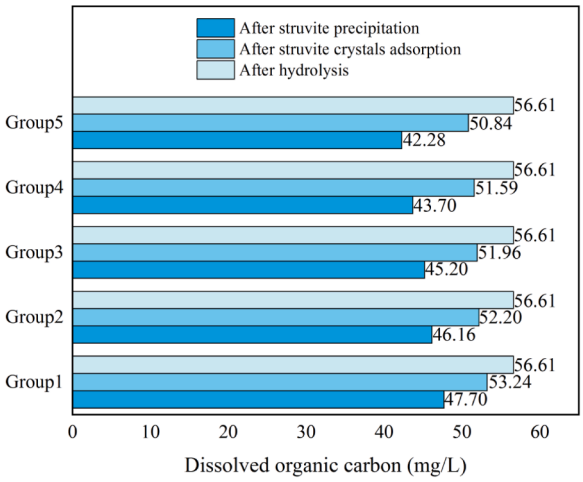

Fig. 10. Variation of DOM concentrations in swine wastewater after three subsequent stages, i.e. hydrolysis, struvite crystal adsorption and struvite precipitation. Struvite crystals of Group 1–5 were 3, 6, 9, 12, and 15 mmol/L during the stage of struvite crystal adsorption, respectively.

Table 4
Contribution of the sub-processes of DOM evolution onto TCs migration during struvite crystallization. Struvite crystals of Group 1–5 were 3, 6, 9, 12, and 15 mmol/L during the stage of struvite crystal adsorption, respectively.

Samples	Event	Contribution percentage (%) OTC	TC	DXC
Group 1	Pure struvite crystals adsorption	3.26%	3.91%	2.29%
	Struvite adsorbing DOM-TCs complex	22.96%	29.68%	23.52%
	DOM aggregation	73.77%	66.41%	74.19%
Group 2	Pure struvite crystals adsorption	4.75%	6.53%	3.34%
	Struvite adsorbing DOM-TCs complex	24.61%	32.54%	23.85%
	DOM aggregation	70.64%	60.93%	72.81%
Group 3	Pure struvite crystals adsorption	2.79%	3.96%	2.37%
	Struvite adsorbing DOM-TCs complex	23.41%	33.26%	27.69%
	DOM aggregation	73.80%	62.78%	69.94%
Group 4	Pure struvite crystals adsorption	3.70%	5.22%	3.13%
	Struvite adsorbing DOM-TCs complex	25.34%	31.05%	30.54%
	DOM aggregation	70.95%	63.73%	66.34%
Group 5	Pure struvite crystals adsorption	3.68%	6.25%	3.71%
	Struvite adsorbing DOM-TCs complex	27.06%	34.66%	32.50%
	DOM aggregation	69.25%	59.09%	63.79%

experimental runs. A strong linear relationship between binding constants of TCs (K_{DOMa}) and aggregated DOM_a was illustrated in Fig. 9, with the correlation coefficient at 0.90–0.92 (Table S5). For TCs complexation, the values of K_{DOMa} located at 1.18–2.10, which indicated that FDOM aggregation contributed more for TCs transport during struvite recovery from wastewater. Such assertion was also supported by the comparison of the data in Table S6.

3.3. *Quantification of the sub-processes of DOM evolution for TCs transport*

As described in above sections, DOM evolution in struvite crystallization included three, respective sub-processes, i.e. hydrolysis, struvite adsorption and aggregation, which resulted in 4.23−5.95% aqueous DOM lost in the adsorption stage and 10.41−16.84% aqueous DOM lost in the aggregation stage (Fig. 10). Such DOM evolution combining with the adsorption of struvite crystals would ignite TCs transport from the aqueous phase to the recovered struvite products. As displayed in Table 4, the adsorption of pure struvite crystal, struvite adsorbing DOM-TCs complex and DOM aggregation approximately accounted for 2.29–6.53%, 23.53–34.66% and 59.09–74.19% of total TCs migration, respectively. These results demonstrated the significance of the sub-

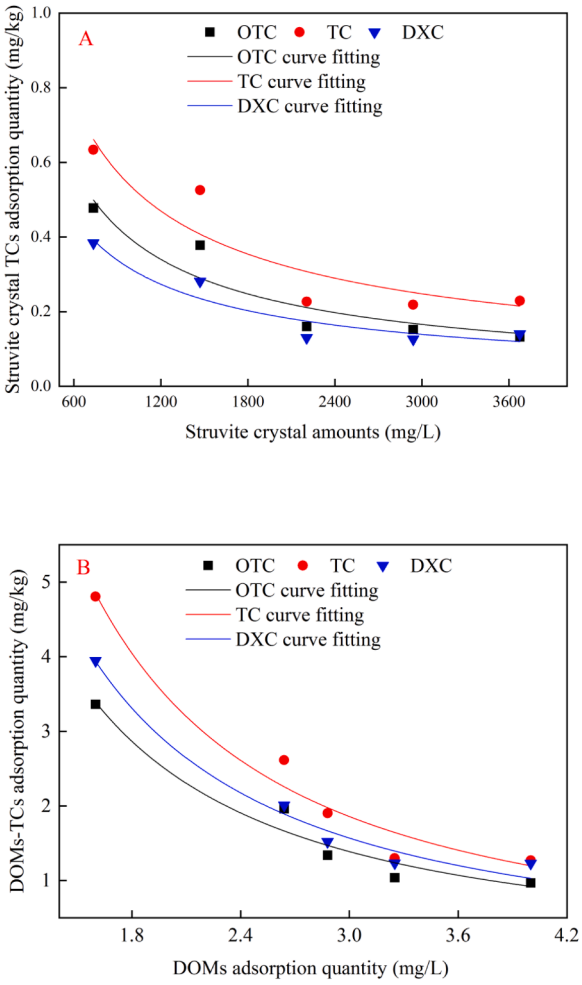

Fig. 11. Regression fitting between struvite crystal TCs adsorption quantity vs struvite crystals amounts (A) and DOMs-TCs adsorption quantity vs DOMs adsorption quantity (B).

processes of DOM evolution driven by struvite crystallization contributing to TCs transport during phosphate recovery from wastewater. Undoubtedly, such data were useful for evaluating the potential eco-risks of antibiotics during struvite recovery from livestock wastewater.

A model concerning TCs mass distributing among different phases, i.e. TCs molecules sorbed to struvite crystals (K_{MAP}), molecules complexing with DOM (DOMs-TCs, K_{DOMs}) adsorbed onto struvite crystals, molecules complexing with DOM aggregated (DOMa-TCs, K_{DOMa}) and molecules freely dissolved in the solution were therefore developed. The coefficients of K_{MAP}, K_{DOMs}, and K_{DOMa} were calculated by regressing TCs adsorption quantity and TCs carrier amounts (Fig. 11), with the detailed deviation listed in Table S7 and S8. Accordingly, the TCs distribution coefficients among various phases, i.e., f_1, f_2, $f_3$and f_4, were therefore determined, as shown in Table 5. To our knowledge, few studies have reported on the characterization of antibiotic distribution in struvite crystallization. Such outcomes were practical for understanding the behavior of antibiotic migration phosphorus recovery from wastewater, which was also good for developing control technology in the near future.

4. Conclusion

This study was conducted to screen out the individual DOM evolution sub-processes on TCs transport and quantified the effects during struvite recovery from swine wastewater. A tangential flow filtration system was employed to divide DOM into five fractional parts on the basis of molecular weight cut-offs. The results suggested that HMW FDOMs such as FDOM1 and FDOM2 had hydrolyzed to LMW FDOMs including FDOM3, FDOM4 and FDOM5 under alkaline conditions, and TCs were redistributed due to the binding power of TCs with HMW DOM becomes weaker. In addition, we speculated that struvite crystal adsorption, DOM-TCs complex and DOM aggregation contributed to TCs migration, which approximately accounted for 2.29–6.53%, 23.53–34.66% and 59.09–74.19%, respectively. Finally, a distribution model was developed to characterize TCs transport by describing TCs distribution among various phases, including struvite adsorption, DOM-TCs complexing, DOM aggregation and free state in the solution, respectively. The outcomes of this study were practical, since it can provide the quantitative information of antibiotic migration during phosphorus recovery. Besides, it will undoubtedly be helpful to develop the methods of antibiotic control in phosphorus recovery from wastewater.

Table 5
TCs distribution coefficient of f_1, f_2, f_3 and f_4 for the adsorption of struvite crystals, DOM-TCs complex adsorption, DOM aggregation and free molecule in the solution, respectively.

TCs	Distribution coefficient	Equations
OTC	f_1	$\frac{88.73C_{MAP}^{-0.78}}{88.73C_{MAP}^{-0.78}+6.62C_{DOMs}^{-1.42}+(2.82C_{DOMa}+0.23)C_{DOMa}+1}$
	f_2	$\frac{6.62C_{DOMs}^{-1.42}}{88.73C_{MAP}^{-0.78}+6.62C_{DOMs}^{-1.42}+(2.82C_{DOMa}+0.23)C_{DOMa}+1}$
	f_3	$\frac{(2.82C_{DOMa}+0.23)C_{DOMa}}{88.73C_{MAP}^{-0.78}+6.62C_{DOMs}^{-1.42}+(2.82C_{DOMa}+0.23)C_{DOMa}+1}$
	f_4	$\frac{1}{88.73C_{MAP}^{-0.78}+6.62C_{DOMs}^{-1.42}+(2.82C_{DOMa}+0.23)C_{DOMa}+1}$
TC	f_1	$\frac{66.69C_{MAP}^{-0.70}}{66.69C_{MAP}^{-0.70}+9.92C_{DOMs}^{-1.18}+(2.77C_{DOMa}+0.24)C_{DOMa}+1}$
	f_2	$\frac{9.92C_{DOMs}^{-1.18}}{66.69C_{MAP}^{-0.70}+9.92C_{DOMs}^{-1.18}+(2.77C_{DOMa}+0.24)C_{DOMa}+1}$
	f_3	$\frac{(2.77C_{DOMa}+0.24)C_{DOMa}}{66.69C_{MAP}^{-0.70}+9.92C_{DOMs}^{-1.18}+(2.77C_{DOMa}+0.24)C_{DOMa}+1}$
	f_4	$\frac{1}{66.69C_{MAP}^{-0.70}+9.92C_{DOMs}^{-1.18}+(2.77C_{DOMa}+0.24)C_{DOMa}+1}$
DXC	f_1	$\frac{51.57C_{MAP}^{-0.74}}{51.57C_{MAP}^{-0.74}+7.83C_{DOMs}^{-1.46}+(3.56C_{DOMa}--0.33)C_{DOMa}+1}$
	f_2	$\frac{7.83C_{DOMs}^{-1.46}}{51.57C_{MAP}^{-0.74}+7.83C_{DOMs}^{-1.46}+(3.56C_{DOMa}--0.33)C_{DOMa}+1}$
	f_3	$\frac{(3.56C_{DOMa}--0.33)C_{DOMa}}{51.57C_{MAP}^{-0.74}+7.83C_{DOMs}^{-1.46}+(3.56C_{DOMa}--0.33)C_{DOMa}+1}$
	f_4	$\frac{1}{51.57C_{MAP}^{-0.74}+7.83C_{DOMs}^{-1.46}+(3.56C_{DOMa}--0.33)C_{DOMa}+1}$

Declaration of Competing Interest

The authors declare that they have no known competing financial interests or personal relationships that could have appeared to influence the work reported in this paper.

Acknowledgment

This work was supported by the General Project of National Natural Science Foundation of China (No. 51878639).

Supplementary materials

Supplementary material associated with this article can be found, in the online version, at doi:10.1016/j.watres.2021.117756.

References

Baalousha, M., Motelica-Heino, M., Coustumer, P.L., 2006. Conformation and size of humic substances: effects of major cation concentration and type, pH, salinity, and residence time. Colloids Surf. Physicochem. Eng. Asp. 272, 48–55. https://doi.org/10.1016/j.colsurfa.2005.07.010.

Bai, L., Zhao, Z., Wang, C., Wang, C., Liu, X., Jiang, H., 2017. Multi-spectroscopic investigation on the complexation of tetracycline with dissolved organic matter derived from algae and macrophyte. Chemosphere 187, 421–429. https://doi.org/10.1016/j.chemosphere.2017.08.112.

Ben, W., Pan, X., Qiang, Z., 2013. Occurrence and partition of antibiotics in the liquid and solid phases of swine wastewater from concentrated animal feeding operations in Shandong Province, China. Environ. Sci. Process. Impacts 15, 870–875. https://doi.org/10.1039/c3em30845f.

Cai, J., Ye, Z.L., Ye, C., Ye, X., Chen, S., 2020. Struvite crystallization induced the discrepant transports of antibiotics and antibiotic resistance genes in phosphorus recovery from swine wastewater. Environ. Pollut. 266, 115361 https://doi.org/10.1016/j.envpol.2020.115361.

Chen, Q.L., An, X.L., Zhu, Y.G., Su, J.Q., Gillings, M.R., Ye, Z.L., Cui, L., 2017a. Application of struvite alters the antibiotic resistome in soil, rhizosphere, and phyllosphere. Environ. Sci. Technol. 51, 8149–8157. https://doi.org/10.1021/acs.est.7b01420.

Chen, W., Yu, H.Q., 2020. Advances in the characterization and monitoring of natural organic matter using spectroscopic approaches. Water Res. 190, 116759 https://doi.org/10.1016/j.watres.2020.116759.

Chen, Y., Jiang, X., Xiao, K., Shen, N., Zeng, R.J., Zhou, Y., 2017b. Enhanced volatile fatty acids (VFAs) production in a thermophilic fermenter with stepwise pH increase-Investigation on dissolved organic matter transformation and microbial community shift. Water Res. 112, 261–268. https://doi.org/10.1016/j.watres.2017.01.067.

Chen, Z., Li, M., Wen, Q., Ren, N., 2017c. Evolution of molecular weight and fluorescence of effluent organic matter (EfOM) during oxidation processes revealed by advanced spectrographic and chromatographic tools. Water Res. 124, 566–575. https://doi.org/10.1016/j.watres.2017.08.006.

Cheng, D., Ngo, H.H., Guo, W., Chang, S.W., Nguyen, D.D., Liu, Y., Wei, Q., Wei, D., 2020. A critical review on antibiotics and hormones in swine wastewater: water pollution problems and control approaches. J. Hazard. Mater. 387, 121682 https://doi.org/10.1016/j.jhazmat.2019.121682.

Ding, Y., Teppen, B.J., Boyd, S.A., Li, H., 2013. Measurement of associations of pharmaceuticals with dissolved humic substances using solid phase extraction. Chemosphere 91, 314–319. https://doi.org/10.1016/j.chemosphere.2012.11.039.

Gu, C., Karthikeyan, K.G., Sibley, S.D., Pedersen, J.A., 2007. Complexation of the antibiotic tetracycline with humic acid. Chemosphere 66, 1494–1501. https://doi.org/10.1016/j.chemosphere.2006.08.028.

Guillossou, R., Le Roux, J., Mailler, R., Pereira-Derome, C.S., Varrault, G., Bressy, A., Vulliet, E., Morlay, C., Nauleau, F., Rocher, V., Gasperi, J., 2020. Influence of dissolved organic matter on the removal of 12 organic micropollutants from wastewater effluent by powdered activated carbon adsorption. Water Res. 172, 115487 https://doi.org/10.1016/j.watres.2020.115487.

Huang, X., Liu, C., Li, K., Liu, F., Liao, D., Liu, L., Zhu, G., Liao, J., 2013. Occurrence and distribution of veterinary antibiotics and tetracycline resistance genes in farmland soils around swine feedlots in Fujian Province, China. Environ. Sci. Pollut. Res. 20, 9066–9074. https://doi.org/10.1007/s11356-013-1905-5.

Kitis, M., Kilduff, J.E., Karanfil, T., 2001. Isolation of dissolved organic matter (dom) from surface waters using reverse osmosis and its impact on the reactivity of dom to formation and speciation of disinfection by-products. Water Res. 35, 2225–2234. https://doi.org/10.1016/S0043-1354(00)00509-1.

Li, B., Dong, S., Huang, Y., Li, P., Yu, W., Wang, G., Young, B., 2021a. Toward a decision support framework for sustainable phosphorus management: a case study of China. J. Clean. Prod. 279, 123441 https://doi.org/10.1016/j.jclepro.2020.123441.

Li, D., Zhou, Y., Tan, Y., Pathak, S., Majid, M.A., Ng, W.J., 2016. Alkali-solubilized organic matter from sludge and its degradability in the anaerobic process. Bioresour. Technol. 200, 579–586. https://doi.org/10.1016/j.biortech.2015.10.083.

Li, J., Wang, X., Wang, Y., Xia, S., Zhao, J., 2021b. Insight into the co-adsorption behaviors and interface interactions mechanism of chlortetracycline and lead onto struvite loaded diatomite. J. Hazard. Mater. 405, 124210 https://doi.org/10.1016/j.jhazmat.2020.124210.

Liu, J., Zhang, P., Tian, Z., Xu, R., Wu, Y., Song, Y., 2020. Pollutant removal from landfill leachate via two-stage anoxic/oxic combined membrane bioreactor_ Insight in organic characteristics and predictive function analysis of nitrogen-removal bacteria. Bioresour. Technol. 317, 124037 https://doi.org/10.1016/j.biortech.2020.124037.

Lou, Y., Ye, Z.L., Chen, S., Wei, Q., Zhang, J., Ye, X., 2018. Influences of dissolved organic matters on tetracyclines transport in the process of struvite recovery from swine wastewater. Water Res. 134, 311–326. https://doi.org/10.1016/j.biortech.2020.124037.

Lu, X., Huang, Z., Liang, Z., Li, Z., Yang, J., Wang, Y., Wang, F., 2021. Co-precipitation of Cu and Zn in precipitation of struvite. Sci. Total Environ. 764, 144269 https://doi.org/10.1016/j.scitotenv.2020.144269.

Ma, D., Gao, B., Sun, S., Wang, Y., Yue, Q., Li, Q., 2013. Effects of dissolved organic matter size fractions on trihalomethanes formation in MBR effluents during chlorine disinfection. Bioresour. Technol. 136, 535–541. https://doi.org/10.1016/j.biortech.2013.03.002.

Ma, S., Hu, H., Wang, J., Liao, K., Ma, H., Ren, H., 2019. The characterization of dissolved organic matter in alkaline fermentation of sewage sludge with different pH for volatile fatty acids production. Water Res. 164, 114924 https://doi.org/10.1016/j.watres.2019.114924.

Moody, C.S., 2020. A comparison of methods for the extraction of dissolved organic matter from freshwaters. Water Res. 184, 116114 https://doi.org/10.1016/j.watres.2020.116114.

Muhmood, A., Wang, X., Dong, R., Wu, S., 2021. New insights into interactions of organic substances in poultry slurry with struvite formation: an overestimated concern? Sci. Total Environ. 751, 141789 https://doi.org/10.1016/j.scitotenv.2020.141789.

NBSPRC, 2020. The China Statistical Yearbook - Number of Livestock (2020). Available online: http://www.stats.gov.cn/tjsj/ndsj/2020/indexch.htm. (Accessed 15 July 2021).

Pan, B., Ghosh, S., Xing, B., 2008. Dissolved organic matter conformation and its interaction with pyrene as affected by water chemistry and concentration. Environ. Sci. Technol. 42, 1594–1599. https://doi.org/10.1021/es702431m.

Safiur Rahman, M., Whalen, M., Gagnon, G.A., 2013. Adsorption of dissolved organic matter (DOM) onto the synthetic iron pipe corrosion scales (goethite and magnetite): effect of pH. Chem. Eng. J. 234, 149–157. https://doi.org/10.1016/j.cej.2013.08.077.

Vanotti, M.B., Dube, P.J., Szogi, A.A., García-González, M.C., 2017. Recovery of ammonia and phosphate minerals from swine wastewater using gas-permeable membranes. Water Res. 112, 137–146. https://doi.org/10.1016/j.watres.2017.01.045.

Van, T.T.H., Yidana, Z., Smooker, P.M., Coloe, P.J., 2020. Antibiotic use in food animals worldwide, with a focus on Africa: pluses and minuses. J. Glob. Antimicrob. Resist. 20, 170–177. https://doi.org/10.1016/j.jgar.2019.07.031.

Wang, Y., Wang, X., Li, J., Li, Y., Liu, Y., Wang, F., Zhao, J., 2020. Adsorption and precipitation behaviors of zinc, copper and tetracycline with struvite products obtained by phosphorus recovery from swine wastewater. J. Environ. Chem. Eng. 8, 104488 https://doi.org/10.1016/j.jece.2020.104488.

Wang, Y., Wang, X., Li, J., Li, Y., Xia, S., Zhao, J., Minale, T.M., Gu, Z., 2019. Coadsorption of tetracycline and copper(II) onto struvite loaded zeolite-an environmentally friendly product recovered from swine biogas slurry. Chem. Eng. J. 371, 366–377. https://doi.org/10.1016/j.cej.2019.04.058.

Xu, H., Lin, H., Jiang, H., Gao, L., 2018. Dynamic molecular size transformation of aquatic colloidal organic matter as a function of pH and cations. Water Res. 144, 543–552. https://doi.org/10.1016/j.watres.2018.07.075.

Xu, L., Zhang, H., Xiong, P., Zhu, Q., Liao, C., Jiang, G., 2021. Occurrence, fate, and risk assessment of typical tetracycline antibiotics in the aquatic environment: a review. Sci. Total Environ. 753, 141975 https://doi.org/10.1016/j.scitotenv.2020.141975.

Ye, Z.L., Deng, Y., Lou, Y., Ye, X., Chen, S., 2018. Occurrence of veterinary antibiotics in struvite recovery from swine wastewater by using a fluidized bed. Front. Environ. Sci. Eng. 12, 1–7. https://doi.org/10.1007/s11783-018-1015-1.

Ye, Z.L., Deng, Y., Lou, Y., Ye, X., Zhang, J., Chen, S., 2017. Adsorption behavior of tetracyclines by struvite particles in the process of phosphorus recovery from synthetic swine wastewater. Chem. Eng. J. 313, 1633–1638. https://doi.org/10.1016/j.cej.2016.11.062.

Ye, Z.L., Zhang, J., Cai, J., Chen, S., 2020. Investigation of tetracyclines transport in the presence of dissolved organic matters during struvite recovery from swine wastewater. Chem. Eng. J. 385, 123950 https://doi.org/10.1016/j.cej.2019.123950.

Yuan, D., Zhao, Y., Guo, X., Zhai, L., Wang, X., Wang, J., Cui, Y., He, L., Yan, C., Kou, Y., 2020. Impact of hydrophyte decomposition on the changes and characteristics of dissolved organic matter in lake water. Ecol. Indic. 116, 106482 https://doi.org/10.1016/j.ecolind.2020.106482.

Zeng, Z., Zheng, P., Ding, A., Zhang, M., Abbas, G., Li, W., 2017. Source analysis of organic matter in swine wastewater after anaerobic digestion with EEM-PARAFAC. Environ. Sci. Pollut. Res. 24, 6770–6778. https://doi.org/10.1007/s11356-016-8324-3.

Zhang, M., Liu, Y.S., Zhao, J.L., Liu, W.R., He, L.Y., Zhang, J.N., Chen, J., He, L.K., Zhang, Q.Q., Ying, G.G., 2018. Occurrence, fate and mass loadings of antibiotics in

two swine wastewater treatment systems. Sci. Total Environ. 639, 1421–1431. https://doi.org/10.1016/j.scitotenv.2018.05.230.

Zhao, P., Zhao, Y., Cui, L., Tian, Y., Zhang, Z., Zhu, Q., Zhao, W., 2021. Multiple antibiotics distribution in drinking water and their co-adsorption behaviors by different size fractions of natural particles. Sci. Total Environ. 775, 145846 https://doi.org/10.1016/j.scitotenv.2021.145846.

Zhou, Q., Li, X., Lin, Y., Yang, C., Tang, W., Wu, S., Li, D., Lou, W., 2019. Effects of copper ions on removal of nutrients from swine wastewater and on release of dissolved organic matter in duckweed systems. Water Res. 158, 171–181. https://doi.org/10.1016/j.watres.2019.04.036.